



Mineralogical characterization of fluorescent grossular garnet var. tsavorite from Merelani Hills, Tanzania

Alfredo Idini¹ · Celestino Angeli² · Franco Frau¹ · Guido Ennas¹ · Stefano Naitza¹ · Giovanni Battista De Giudici¹ · Roberto Argazzi³

Received: 24 June 2022 / Accepted: 17 January 2023
© The Author(s) 2023

Abstract

Tsavorite is the trade name for the green vanadium–chromium variety of grossular occurring in the Precambrian terrains in the areas of Merelani Hills (Tanzania) and Tsavo Park (Kenya) which are by far the most important source of gem grade specimens of tsavorite used for high jewellery. The tsavorite crystals from Merelani Hills exhibit a pink-red and yellow fluorescence when irradiated by common portable UV lamp, an unusual phenomenon among members of the garnet group. The electron density map calculated from the diffraction data and plotted against a grossular standard shows that an excess of negative charge is clearly pinpointed in the crystallographic site occupied by Al³⁺. The bulk elemental analysis shows that the most represented end-member, besides grossular, is the vanadium-bearing goldmanite garnet (3.82–4.08 mol %). The fluorometry with an excitation beam at 408 nm indicates a complex emission pattern with the most intense emissions at 701 and 716 nm and subordinately at 592 nm. The colour perception is dominated by the emission yellow band at 592 nm while the contribution of the red band modulates the colour ranging from bright orange to pink-red. The attribution of the emission at 592 nm is related to Mn²⁺ while the emissions at 701 and 716 nm could be related to the chromium content and/or to a possible fraction of vanadium as V²⁺. Because of the characteristic colour perceived under UV light, the use of a common led lamp can be useful as a diagnostic tool to easily identify tsavorite.

Keywords Tsavorite · Vanadium grossular · Garnet fluorescence · Merelani Hills (Tanzania) · Electron density map · Natural photoluminescence

Introduction

The general formula for the garnet supergroup minerals is {X₃}[Y₂](Z₃)φ₁₂, where X, Y, and Z refer to dodecahedral, octahedral, and tetrahedral sites, respectively, and φ is O, OH, or F (Grew et al. 2013). In addition to the 32 species of garnet, there are many variety names as in case of tsavorite which is the trade name for the green vanadium–chromium

variety of grossular that ideally follows the formula Ca₃(Al,V,Cr)₂(SiO₄)₃ (Feneyrol et al. 2013). Although tsavorite is not a mineral species approved by the International Mineral Association (Grew et al. 2013), we will use this term for the sake of consistency with the actual literature on this topic. The first documented occurrence of tsavorite dates back to late 1960s (Bridges 1974) in north-east Tanzania. Other noticeable occurrences of tsavorite, in term of size and quality of the crystals, have been documented in few localities: Tsavo Park, Kenya (Bridges 1974), Swat Valley, Pakistan (Jackson 1992), Gogogo area and near Itrafo village in Madagascar (Adamo et al. 2012), and in Sør Rondane Mountains, Antarctica (Osanaï et al. 1990). The areas of Merelani Hills (Tanzania) and Tsavo Park (Kenya) are the most important sources of gem grade specimens of tsavorite used for high jewellery (Cairncross 2020). Due to the popularity and commercial value of tsavorite, its price has raised up to ~8000 € per carat for top-grade faceted gems and tsavorite is present in the catalogue of many luxury companies.

✉ Franco Frau
frau@unica.it

¹ Department of Chemical and Geological Sciences, University of Cagliari, Cagliari, Italy

² Department of Chemical, Pharmaceutical and Agricultural Sciences, University of Ferrara, Ferrara, Italy

³ Department of Chemical, Pharmaceutical and Agricultural Sciences, Institute for Organic Synthesis and Photoreactivity, National Research Council (ISOF-CNR), University of Ferrara, Ferrara, Italy

Beyond the importance as a gem, tsavorite plays a key role in the geological and petrological research because it is hosted exclusively in the metamorphic unit from the Neoproterozoic Metamorphic Mozambique Belt (NMMB) (Feneyrol et al. 2013). The petrological studies of the tsavorite deposit of the NMMB have allowed to determine the composition of the protoliths and their metamorphic evolution (Feneyrol et al. 2012, 2014; Jacob et al. 2018), contributing to the geological studies related to the formation of Gondwana continent. Furthermore, the tsavorite crystals exhibit a peculiar feature: an orange-pink and yellow fluorescence under long-wave and short-wave UV, respectively. This phenomenon is unusual among the members of the garnet group and, to the best of our knowledge, only few research papers have investigated the luminescence in natural garnets in the range of visible light, while for synthetic garnet, such as the Yttrium Aluminium Garnet (YAG), there is a number of studies due to its importance in technology fields as phosphor (Xia and Meijerink 2017). In one of the oldest papers (Mazurak and Czaja 1995), the role of Cr^{3+} and V^{3+} activation centres has been supposed to be the source of luminescence in natural grossular. However, other different activation centres are supposed to contribute to the photoluminescence (Gaft et al. 2013). Taking into account the various field of interest mentioned in which tsavorite occupies a prominent place, the general aim of this work is to contribute to the mineralogical studies of the tsavorite from Merelani Hills (Tanzania) through the following specific objectives: (i) acquisition of luminescence spectrum with emphasis on the output in the visible light range; (ii) acquisition of high-resolution PXRD (powder X-ray diffraction) pattern and subsequent analysis through

the Fourier electron density map; (iii) elemental chemical composition and interpretation of the crystal chemistry.

For the avoidance of doubt as to the ultimate purpose of this study, we would like to make it clear that it is not our intention to present a detailed analysis of the spectroscopic characteristics of tsavorite, but rather to perform, in addition to a purely mineralogical (crystallographic and crystallochemical) study, an analysis of the spectroscopic response of tsavorite in the visible spectrum, comparing our results with those found in the literature, in an attempt to put a definitive point in the myriad of dispersed, contradictory and inhomogeneous data.

Materials and methods

Tsavorite samples

The tsavorite specimens were acquired from the miners outside the D-Block mine, Merelani Hills, Manyara Region, Tanzania. As described by Feneyrol et al. (2010) and following our field observations, the paragenesis of the samples is composed by tsavorite hosted in graphitic gneiss in association with diopside, zoisite var. tanzanite, pyrite and scapolite. The samples used for the luminescence observation were carefully handpicked looking for most euhedral and inclusion-free crystals (Fig. 1). Two sets of crystals of 20 g each were selected under the UV lamp and then crushed in an agate mortar to perform the PXRD acquisition. After that, the same powder was submitted to the laboratory for the elemental analysis. The UV light observations of red and



Fig. 1 Deep green tsavorite crystals, from 3 to 8 mm, hosted in graphitic gneiss. The quality of the crystals in figure are representative of the samples handpicked for analysis

yellow colours of the selected crystals were made with two handheld lamps with peak wavelength emissions at 405 nm and 280 nm (Fig. 2).

Analytical techniques

Emission and excitation spectra were recorded with an Edinburgh Instruments FS920 steady state spectrofluorometer configured with a 450 W xenon short arc lamp as excitation source, a TMS300-X single excitation monochromator supplied with a 1800 g/mm grating blazed at 250 nm (300 mm focal length, $f/4.1$ aperture, 1.8 nm/mm linear dispersion), a double emission monochromator consisting of two coupled 300 mm focal length, $f/4.1$ monochromators supplied with 1200 g/mm gratings blazed at 500 nm (1.35 nm/mm linear dispersion) and a universal sample chamber. A red sensitive photomultiplier (Hamamatsu R928P) in a standard uncooled housing mounted at the exit port of the second stage of the emission monochromator was used as detector in the 200–850 nm wavelength interval. Crystal specimens (typically 3–4 mm in diameter) were mounted on a front face sample holder inclined at 30° with respect to the vertical axis and horizontally adjustable through a linear stage from outside the sample chamber. Using the linear adjustment, the sample was precisely positioned at the intersection of the excitation and emission paths to maximize intensity. The instrument was PC controlled through a proprietary Edinburgh Instruments F900 software providing emission and excitation spectra factory corrected for instrument response by means of a calibrated source. The contribution to the acquired signal due to the excitation monochromator stray light, for each excitation and emission slits selected, was checked both with a PTFE and a BaSO_4 diffuser. The PXRD pattern was collected by a PANalytical X'Pert Pro diffractometer equipped with an X'Celerator[®] detector operating at 40 kV and 40 mA in the Bragg – Brentano θ – θ geometry using $\text{Cu-K}_{\alpha 1}$ radiation ($\lambda = 1.54060 \text{ \AA}$) in the range of 5 – 120° (2θ) with a step size of 0.008° (2θ) and 45 s time per step equivalent to 180 h of acquisition time. Using the

X'Celerator detector, based on Real Time Multiple Strip technology of the 128 mounted detectors, the effective acquisition time was 1 h 24 min. The software used for the mineralogical analysis and interpretation was X'Pert High-Score Plus version 2.12b (Degen et al. 2014). In order to recast the analyses of garnet into end-member components, the spreadsheet proposed by Locock (2008) has been used. The chemical analysis using ICP-AES (Inductively Coupled Plasma Atomic Emission Spectroscopy) was performed by ALS Laboratory group, an INAB accredited laboratory Reg. No. 173 T that meets the general requirements of the ISO/IEC 17025:2017.

Results

Tsavorite fluorescence

Photoluminescence properties of tsavorite crystal specimens were investigated by steady state fluorometry at room temperature. The emission spectrum recorded with an excitation beam at 408 nm is shown in Fig. 3. Two distinct broad emission bands of comparable intensity were observed in the 500–800 nm wavelength range: a higher energy featureless band centred at 592 nm with 66 nm half-width and a lower energy, slightly broader band with two main sharper peaks superimposed at 701 nm and 716 nm. The excitation spectrum of the 592 nm emission band (Fig. 3, blue line) resulted in a profile consisting of three intense, well resolved and almost equally spaced in wavelength, peaks at 408, 419 and 429 nm, followed by two broader bands of lower intensity at higher wavelengths with maxima at 451 nm and 474 nm. The emission bands shown in Fig. 3 are sufficiently spaced apart to allow recording of excitation spectra, at the peak emission wavelength of the two bands, without significant overlap of the corresponding excitation profiles. In Fig. 4, the excitation spectrum of the 716 nm emission band is reported showing two absorption bands of almost equal intensity at 442 nm and 603 nm.



Fig. 2 Same tsavorite crystal, 1.4 cm size, under white LED light (left), 405 nm longwave UV light (middle) and 280 nm shortwave UV light (right)

Fig. 3 Emission spectrum (red line) obtained exciting at 408 nm and excitation spectrum (blue line) of the 592 nm emission of a tsavorite crystal sample

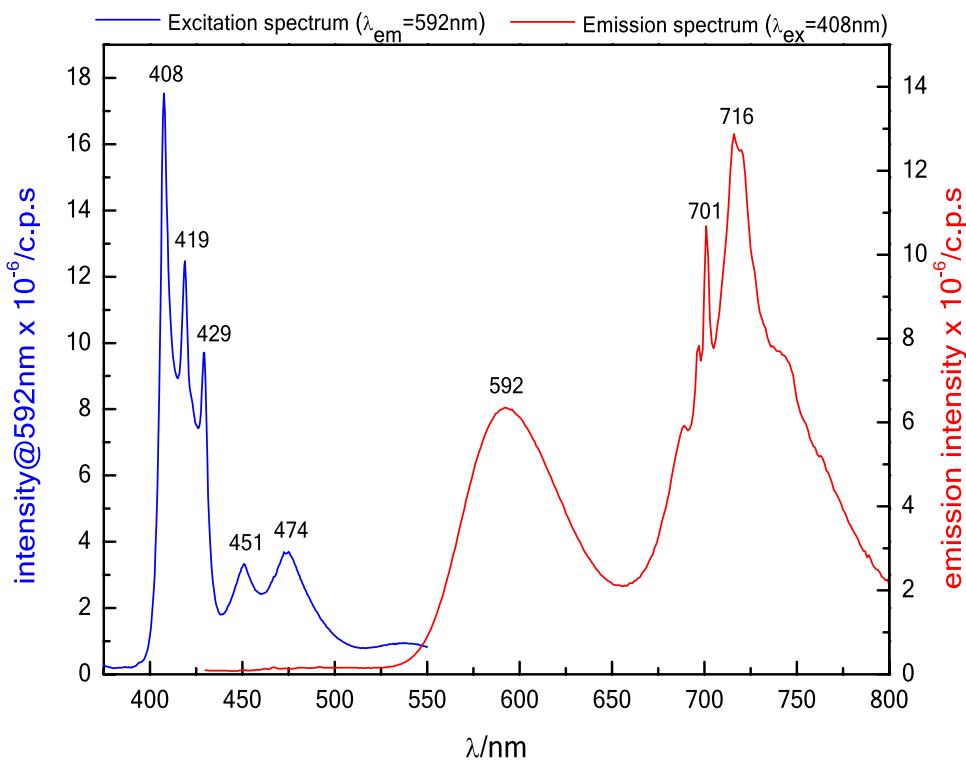
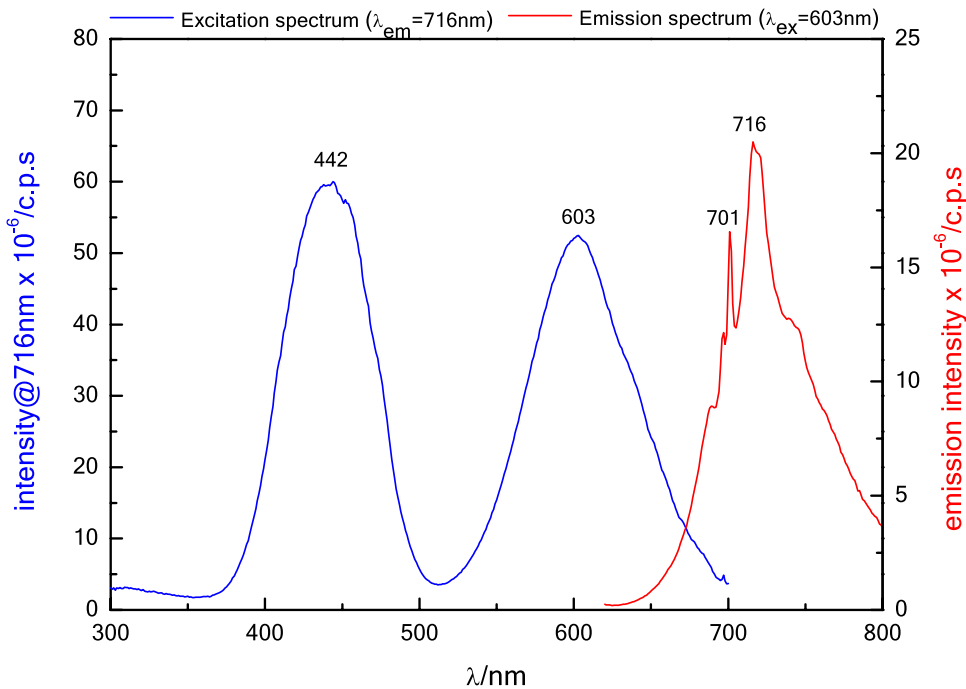


Fig. 4 Emission spectrum (red line) obtained exciting at 603 nm and excitation spectrum (blue line) of the 716 nm emission of a tsavorite crystal sample



As shown in Fig. 5, the colour perception of the light emitted by tsavorite crystals after UV excitation is dominated by the emission band at 592 nm which is close to the peak sensitivity of the human eye at 555 nm, while

the contribution of the red band, though more intense, is perceived as much weaker due to the lower eye sensitivity and modulates the colour ranging from bright orange to orange-red depending on the excitation wavelength.

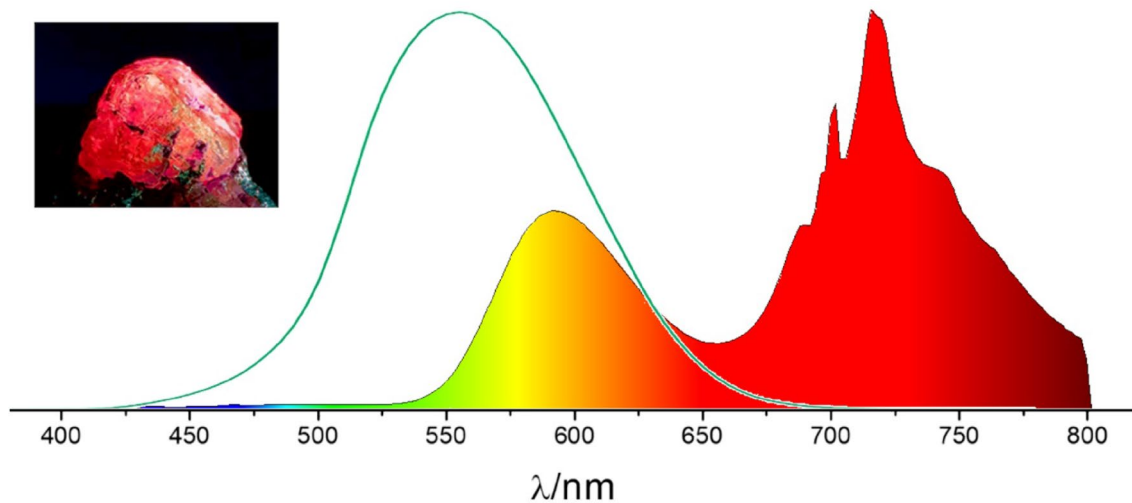


Fig. 5 Tsavorite crystal under led UV light $\lambda \sim 400$ nm (upper left image) and its spectrum with colour distribution recorded with a 408 nm excitation beam compared with the photopic eye sensitivity curve (green line)

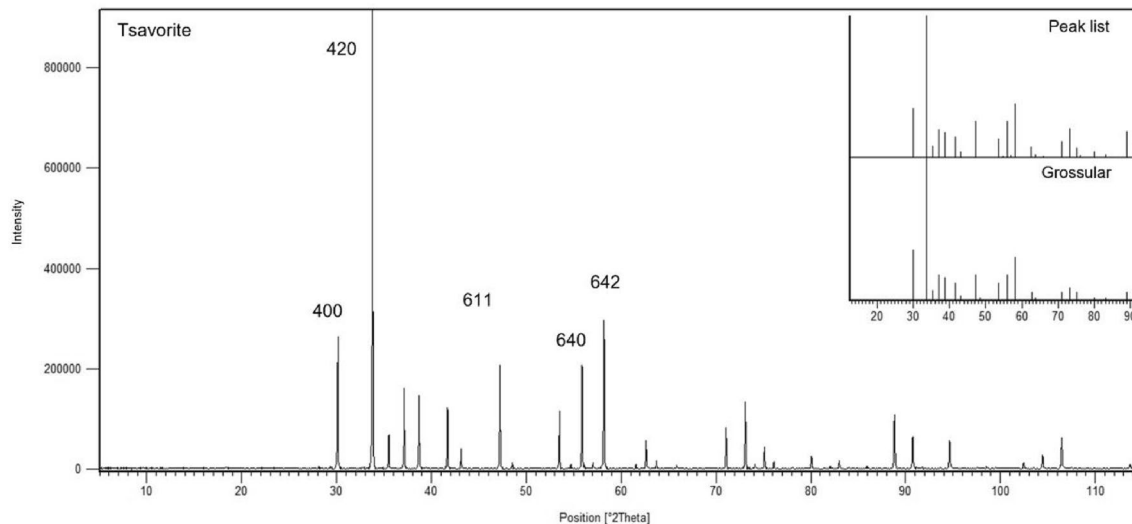


Fig. 6 PXRD pattern of tsavorite. Peaks position from the experimental pattern and reflections from grossular (reference pattern PDF-2 n. 039–0368) are compared in the upper-right box

Tsavorite crystallography

The PXRD pattern of tsavorite is shown in Fig. 6. The peaks position and intensity confirm that garnet is the only phase recognizable in the sample. Among the members of the garnet group, the best fit refers to natural grossular (reference pattern PDF-2 n. 039–0368; Keller et al. 1987).

No reference pattern of tsavorite is present in the international databases (i.e., ICDD, AMCD, ICSD, COD and RUFF™). Because of that, the co-presence of other garnet end-members, such as uvarovite $\text{Ca}_3\text{Cr}_2(\text{SiO}_4)_3$ and goldmanite $\text{Ca}_3\text{V}_2(\text{SiO}_4)_3$, should be considered carefully

due to the reflections overlap of these species. The reflections indexing and unit-cell parameters have been calculated using both the McMaille (Le Bail 2004) and the DICVOL04 (Boultif and Louër 2004) algorithms. The results, summarized in Table 1, show that the tsavorite parameters ($a = 11.8558(3)$ Å, $V = 1666.430$ 10^6 pm^3 calculated with McMaille algorithm; $a = 11.8560(2)$ Å, $V = 1666.520$ 10^6 pm^3 calculated with DICVOL04 algorithm) point out to the cubic crystal system (space group $Ia\bar{3}d$), and the parameters are slightly larger than both natural and synthetic grossular lattices.

Table 1 Experimental lattice parameters of tsavorite compared with those of grossular from the literature

Sample	Method	N	N_{poss}	Unindexed reflection	Minimum relative intensity	$a = b = c$ (Å)	$\alpha = \beta = \gamma$ (°)	V (10^6 pm^3)	Space Group	FoM*	References
Tsavorite	McMaille	48	170	0	0.05	11.8558(3)	90	1666.430	Ia-3d	30.6395	This work
Tsavorite	DICVOL04	38	170	0	0.63	11.8560(2)	90	1666.520	Ia-3d	45.5240	This work
Synthetic grossular		44		0	1	11.8470	90	1662.743	Ia-3d		Geiger and Armbruster (1997)

N diffraction lines observed; N_{poss} possible diffraction lines

*Figure of Merit, according to Smith and Snyder (1979)

The Figure of Merit (FoM) of the refined unit-cell parameters was calculated as follows (Smith and Snyder 1979):

$$\text{FoM} = \frac{1}{\Delta 2\theta} \frac{N}{N_{\text{poss}}}, \quad (1)$$

where N_{poss} is the number of possible diffraction lines up to the N observed line and $\Delta 2\theta$ is the average absolute discrepancy between the observed and calculated 2θ values. The FoM = 30.64 calculated via McMaille method indicates an average discrepancy of 0.009 2θ for the 48 diffraction lines with minimum intensity of 0.05%. Using DICVOL04 the 2θ discrepancy decreases to 0.005 and thus FoM increases to 45.52 using 38 lines with minimum intensity of 0.63% out of the 170 possible lines. All the raw data scan and the indexed reflections are reported in supplemental data Table SD1.

To highlight the crystallographic features of tsavorite, the electron density maps (also called Fourier maps or electron scatter density map) from the diffraction data were drawn. The choice of the crystallographic model was the starting point. Among the plenty of grossular data in the literature, the CIF (Crystallographic Information File) from synthetic sample has been chosen (Geiger and Armbruster 1997) to avoid the chemical variabilities of the geological samples due, for instance, to inhomogeneous temperature and pressure of crystallization. The atomic coordinates of the synthetic grossular from CIF are reported in Table 2, while 1/8 of the synthetic grossular unit cell is shown in Fig. 7.

The electron density ρ ($\text{e}^- \cdot \text{Å}^{-3}$) in the x, y, z real space can be expressed as summation over all reflections as indicated below:

$$\rho(x, y, z) = \sum_{hkl} F_{hkl} e^{-2\pi i(hx+ky+lz)} / V, \quad (2)$$

where V is the cell volume, F_{hkl} is the structure factor of each hkl reflection and $(hx + ky + lz)$ is the spatial distribution from the phase used as crystal model. Starting from the last-square fitting profile, through Rietveld algorithm, the observed (F_{obs}) and calculated (F_{calc}) structure factors for each hkl reflection have been derived (supplemental data Table SD1). Finally, the electron density ρ can be expressed as

$$\rho(x, y, z) = \frac{\sum_{hkl} \{F_{hkl \text{ obs}} - F_{hkl \text{ calc}}\} e^{-2\pi i(hx+ky+lz)}}{V}. \quad (3)$$

A significative difference in the $F_{\text{obs}} - F_{\text{calc}}$ Fourier map has been found in the Y site at the vertices and in the centre of the cell. The respective map of the layer $x, y, z = 0$ (Fig. 8), represented by the solid black square in Fig. 7, indicates an increment of the electron density of $2.67 \text{ e}^- \cdot \text{Å}^{-3}$ in the Wyckoff position 16a with respect to the grossular model, where that position is occupied only by Al^{3+} .

Table 2 Atomic coordinates, isotropic atomic displacement parameters B_{iso} (Å²), site occupancies of synthetic grossular used for comparison with tsavorite

Element	Crystallographic site (coordination number)	x	y	z	B_{iso}	Occupancy	Wyckoff position
Ca ²⁺	X (12)	1/8	0	1/4	0.445	1	24c
Al ³⁺	Y (6)	0	0	0	0.365	1	16a
Si ⁴⁺	Z (4)	3/8	0	1/4	0.328	1	24d
O ²⁻		0.03823	0.04528	0.65137	0.411	1	96h

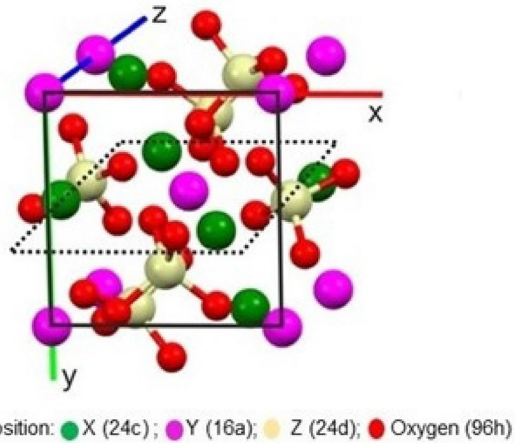
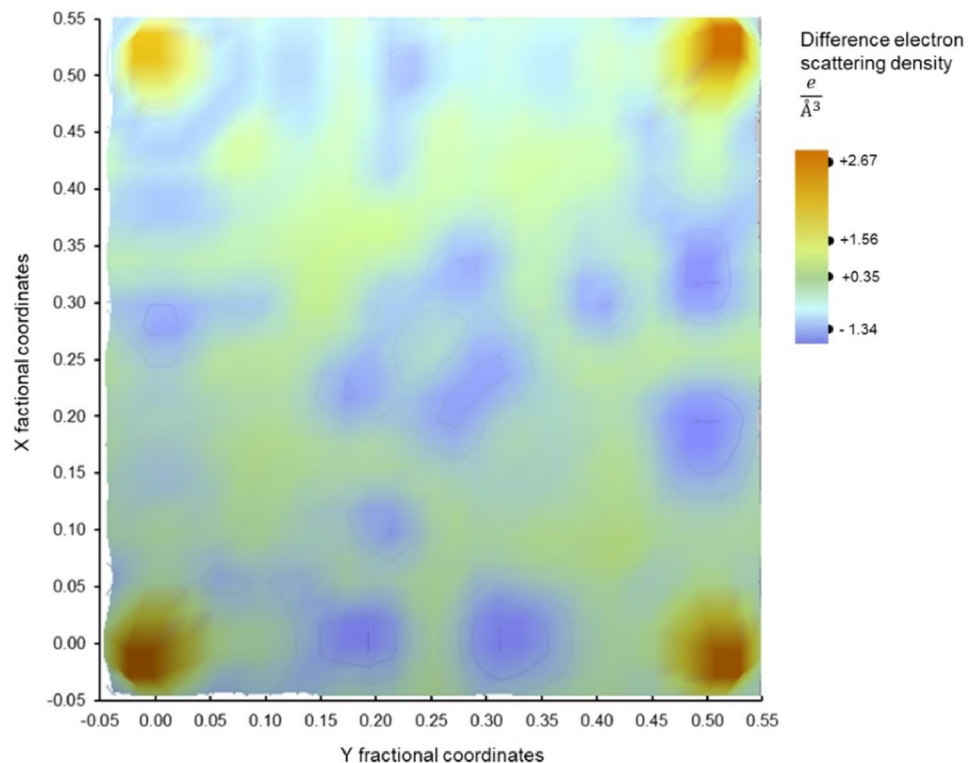


Fig. 7 The drawing shows 1/8 of the synthetic grossular unit cell and the two intersecting planes (solid and dotted black squares) where the Fourier maps of tsavorite show significant differences compared to the grossular model

Fig. 8 Difference Fourier map (Fobs–Fcalc) of the layer $x, y, z=0$. The Y site at the vertices of the map shows an electron scattering density ($2.67 \text{ e} \cdot \text{Å}^{-3}$) higher than that of the grossular model



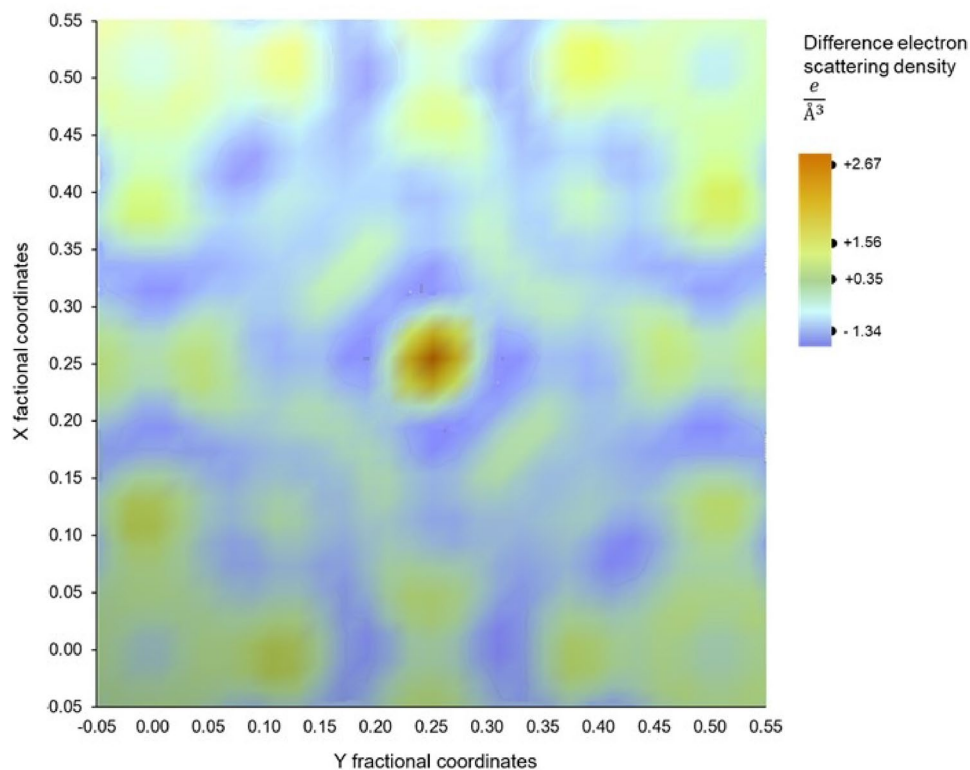
The intersection in the centre of the cell (square with dotted lines in Fig. 7) produces a map (Fig. 9) where the Y site (normally occupied by Al³⁺), for the layer $x, y, z=0.25$, shows again a positive difference of $2.67 \text{ e} \cdot \text{Å}^{-3}$ in the electron density compared to the grossular model.

The information from both maps suggests that some atomic substitution occurs in the Y site. As mentioned in the introduction, Cr³⁺ and/or V³⁺ may replace Al³⁺ in tsavorite and, considering the higher atomic number of both Cr and V compared to Al, this substitution may cause the positive difference in the electron density maps. This hypothesis will be better discussed after the crystal chemistry analysis.

Tsavorite crystal chemistry

The bulk crystal chemistry of the two sets of tsavorite considered in this work (labels Tsavo M and Tsavo T) is reported in Table 3. For comparison, other two bulk analyses

Fig. 9 Difference Fourier map (Fobs–Fcalc) of the layer $x, y, z=0.25$. The Y site at the centre of the map shows an electron scattering density ($2.67 \text{ e}\cdot\text{\AA}^{-3}$) higher than that of the grossular model



of tsavorite from Merelani Hills (Tanzania) are reported in the same table (labels Tsavo L1 and Tsavo L2) (Feneyrol et al. 2013 and reference therein).

In order to recast the analyses of garnet into end-member components, the spreadsheet proposed by Locock (2008) has been used.

To reach the quality index “superior”, as proposed by Locock (2008), at least three out of four of the following parameters must be accomplished: (i) the analytical total inside the range of 97–101%; (ii) the proportions for one or more cation sites must be ideal ($X=3, Y=2, Z=3$); (iii) no octahedral Si if $\text{Mg} < 0.75$ apfu (atoms per formula unit); (iv) the magnitude of the remainder should be $< 1\%$. The remainder is defined as the percentage of the weight that cannot be assigned to an end-member because of the excess of apfu for each cation left over after the calculation of site occupancy. Except for the LOI (loss of ignition) that is measured at 1.47 wt% and 1.23 wt% for Tsavo M and Tsavo T respectively, the elemental analysis of the samples shows a good agreement with the literature data. The amount of the elements other than the main components of grossular are nearly identical in the two samples Tsavo M and Tsavo T, and are in the following order $V > \text{Mg} > \text{Mn} > \text{Ti} > \text{Cr}$ when expressed as oxides, while the Fe content as oxides ranges from 0.12 wt% in Tsavo T to 0.39 wt% in Tsavo M. Taking into account the cation site attributions (Table 4), we observe a very small deficit of Si in the Z site, filled by Al. In the octahedral site (Y), substitution of Al occurs by $V > \text{Ti} >$

$\text{Fe}^{2+} + \text{Fe}^{3+} > \text{Cr}$. Interestingly, all the elements listed above have an atomic number, and therefore, an electron density, greater than Al, and this could be the cause of the difference of the electronic density showed in the electron density maps (Figs. 8 and 9). Concerning the dodecahedral site (X), where no clear differences arise from the electron density maps, the vicariances for Ca are from Mg (0.0401–0.0643 apfu), Mn (0.0215–0.0221 apfu) and Fe^{2+} (0.0017–0.0154 apfu). Taking into account the final apfu calculation, the percentage of each end-member can be expressed as follows (Table 3): grossular $[\text{Ca}_3\text{Al}_2(\text{SiO}_4)_3]$ 91.06–92.84 mol %; goldmanite $[\text{Ca}_3\text{V}_2(\text{SiO}_4)_3]$ 4.08–3.82 mol %; pyrope $[\text{Mg}_3\text{Al}_2(\text{SiO}_4)_3]$ 2.14–1.34 mol %; schorlomite-Al $[\text{Ca}_3\text{Ti}_2((\text{Si}, \text{Al})\text{O}_4)_3]$ 0.86–0.70 mol %; spessartine $[\text{Mn}_3\text{Al}_2(\text{SiO}_4)_3]$ 0.72–0.74 mol %; uvarovite $[\text{Ca}_3\text{Cr}_2(\text{SiO}_4)_3]$ 0.05–0.05 mol % for Tsavo M and Tsavo T, respectively. The attribution of the small amounts of morimotoite $[\text{Ca}_3(\text{TiFe}^{2+})(\text{SiO}_4)_3]$ 0.20–0.33 mol %, almandine $[\text{Fe}_3\text{Al}_2(\text{SiO}_4)_3]$ 0.51–0.06 mol % and andradite $[\text{Ca}_3\text{Fe}_2(\text{SiO}_4)_3]$ 0.39–0.14 mol % are uncertain because these end-members are dependent on the oxidation state of iron.

Discussion

The PXRD pattern of tsavorite shows that no other phases but tsavorite are recognizable in the analysed samples and the atoms are arranged in a cubic structure (space group

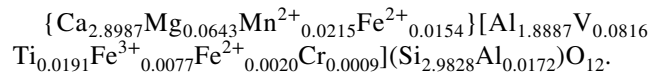
Table 3 Elemental bulk composition and end-member calculation of tsavorite samples, Tsavo M and Tsavo T (this work), and two samples from the literature, Tsavo L1 and Tsavo L2 (Feneyrol et al. 2013)

	Tsavo M	Tsavo T	Tsavo L1	Tsavo L2
Composition (wt%)				
SiO ₂	38.70	38.90	39.69	39.76
TiO ₂	0.33	0.30	0.46	0.43
Al ₂ O ₃	20.98	21.15	20.95	21.70
Cr ₂ O ₃	0.02	0.02	0.29	0.13
V ₂ O ₃	1.32	1.24	1.86	0.63
FeO/FeO _{tot}	0.39	0.12	0.07	0.07
Fe ₂ O ₃ /calc				
MnO	0.33	0.34	0.62	0.72
(Mn ₂ O ₃)				
MgO	0.56	0.35	0.55	0.56
CaO	35.10	35.70	35.98	35.80
Total (calc)	97.73	98.12	100.47	99.80
Recalculated				
Final FeO	0.27	0.08	0.04	0.06
Final Fe ₂ O ₃	0.13	0.05	0.03	0.01
Final MnO	0.33	0.34	0.62	0.72
Final Mn ₂ O ₃	0.00	0.00	0.00	0.00
Total	97.74	98.13	100.47	99.80
End-members (mol%)				
Grossular	91.06	92.84	88.65	92.64
Goldmanite	4.08	3.82	5.61	1.90
Pyrope	2.14	1.34	2.05	2.08
Schorlomite-Al	0.86	0.70	0.79	0.14
Spessartine	0.72	0.74	1.32	1.53
Morimotoite	0.20	0.33	0.22	0.38
Almandine	0.51	0.06	0.01	0.04
Andradite	0.39	0.14	0.08	0.03
Uvarovite	0.05	0.05	0.86	0.39
Remainder	0.00	0.00	0.40	0.87
Total	100.01	100.02	99.99	100
Quality Index	Superior	Superior	Superior	Superior

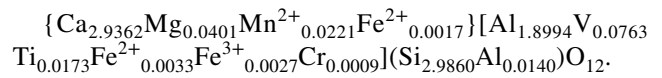
Ia–3d; $V = 1666.430 \text{ 10}^6 \text{ pm}^3$; $a = 11.8558(3) \text{ \AA}$), slightly bigger than synthetic grossular. This consideration was the first sliding door to understand if the fluorescence phenomena belong to the garnet or are possibly generated by other included phases. The second step was the investigation of the atoms displacement, and in the Fourier map, the Wyckoff positions of the cubic system are accomplished. At the same time, a positive difference arises on the electron density between tsavorite and synthetic grossular: this difference is centred in the *Y* (16a) position which is occupied by Al in pure grossular. This positive difference implies that another element with a higher atomic number, and thus a bigger electron density, is substituting for Al. Due to the presence of atomic substitution, the shape

of the octahedral polyhedra of this site could be slightly distorted, shifting the position of oxygen and causing the systematic differences of the small positive/negative density areas of the map in the other positions. The LOI values, unusual for a normally anhydrous mineral, are related to the known H₂S fluid inclusion (Feneyrol et al. 2017) (extremely noticeable during the grinding of the samples due to the characteristic smell) and linked to the graphitic inclusions. Following the cation assignments and apfu calculations (Table 4), the empirical formula of the two sets of tsavorite could be written as follows:

Tsavo M:



Tsavo T:



As mentioned in the introduction, the tsavorite deposits actually occur only in the terrains of the Precambrian NMMB, that is now dislocated in Africa, Asia and South Antarctica. The chemical signature of tsavorite from these deposits is represented by the coexistence of a few hundred mg/kg of Mn, V and Cr and, most importantly, the very small amount of andradite, which is usually the main component of garnets in skarn-type worldwide deposits together with grossular. Feneyrol et al. (2014) proposed a chemical sub-differentiation based on the concentrations of the minor elements Mn, V and Cr. Our samples fall into the Type 2: $V > Mn > Cr$; Type 2 concerns tsavorite from Lemshuku and Merelani, Tanzania (our samples come from Merelani), Tsavo region in Kenya, Madagascar and South Antarctica. Also, the molar V/Cr ratio was proposed to better discriminate the deposit type; in the case of garnet from Merelani (Tanzania) the molar V/Cr ratio is close to 10, but our samples exceed 80. This could be influenced by the fact that we analysed only the gem quality specimens, that usually have a greater amount of V (Cairncross 2020).

The photoluminescence of tsavorite in the visible light is well defined by two regions of the excitation spectrum. The comparison between the excitation spectra obtained for the observed emissions (Fig. 3) clearly shows that there must be at least two chemically distinct activation centres responsible for the luminescence behaviour of the investigated samples. This is further confirmed by recording the emission spectrum exciting at 603 nm where only one of the two emitting centres is activated: in this case only the deep red band is observed (Fig. 4, red line). If excitation occurs in the 400–500 nm interval, both centres strongly absorb simultaneously, leading to the appearance of both emission bands with an intensity ratio determined by their respective absorption.

Table 4 Cation assignment and apfu (atoms per formula unit) calculations for the samples of isavorite Tsavo M and Tsavo T (this work) and two samples from the literature, Tsavo L1 and Tsavo L2 (Feneyrol et al. 2013)

Cations	Cation assignment (apfu)															
	Tsavo M			Tsavo T			Tsavo L1			Tsavo L2						
	Dodecahedral (X)	Octahedral (Y)	Tetrahedral (Z)	Dodecahedral (X)	Octahedral (Y)	Tetrahedral (Z)	Dodecahedral (X)	Octahedral (Y)	Tetrahedral (Z)	Dodecahedral (X)	Octahedral (Y)	Tetrahedral (Z)				
Si	0.0000	0.0000	2.9828	0.0000	0.0000	2.9860	0.0000	0.0000	2.9860	0	0	2.984 (0.0120)	0	0	2.9972 (0.0261)	
Ti		0.0191			0.0173			0.026 (0.0800)					0.0244 (0.0174)			
Al	1.8887		0.0172	1.8994		0.0140				0.0158				1.925		0.0028
Cr	0.0009			0.0009						0.0172				0.0077		
V	0.0816			0.0763						0.1121				0.0381		
Fe ²⁺	0.0154	0.0020		0.0033			0.0003	0.0022			0		0.0038			
Fe ³⁺	0.0077		0.0000	0.0027		0		0.0017		0			0.0006			0
Mn ²⁺	0.0215						0.0395							0.0460		
Mg	0.0643	0.0000		0.0000			0.0616	0						0.063		
Ca	2.8987						2.899 (0.0120)	2.9362						2.8915 (0.261)		
Site Sum	3.0000	2.0000	3.0000	2.0000	2.0000	3.0000	3.0000	2.0000	3.0000	3.0000	2.0000	3.0000	3.0000	2.000	2.000	3.0000
Remainder							0.0120	0.0800		0.012			0.0261		0.0174	
Anions	12.0000						12.040						12.009			

The values in bracket are the remainder apfu not assigned in any crystallographic site

The first activation centre defined by the broad band centred at 592 nm ($\lambda_{\text{ex}} = 408$; Fig. 3) can be assigned to Mn^{2+} that is a well-studied luminescence centre in many minerals (Gaft et al. 2015a). As already mentioned in the crystal chemistry section, the apfu calculations (Table 4) show that all the Mn is assigned to the dodecahedral site (X) as Mn^{2+} , leading to the calculation of spessartine end-member as 0.72–0.74 mol % for Tsavo M and Tsavo T, respectively. It is worth noting that under a 254 nm light the Mn^{2+} is activated (Fig. 10), while the activation centre in the red region has a feeble response. This could be the reason why using portable shortwave UV lamps the crystal appears yellow.

The elemental attribution of the second activation centre, defined by the bands at 697, 701 and 716 nm (Fig. 3), is a bit trickier. The first attribution could be related to the well-known Cr^{3+} emissions.

In one of the oldest papers regarding the luminescence of tsavorite (Mazurak and Czaja 1995) the absorption spectrum reported is very similar to that showed in Fig. 3 and all the emission peaks are attributed to Cr^{3+} . In the book “Luminescent minerals” (Gaft et al. 2015b) it is reported that “The luminescence spectra of Cr^{3+} in grossular at room temperature contain a strong broad band peaking at 720 nm and three sharp lines centred at 697, 700 and 701 nm”. In our experimental patterns, the bands at 701 and 716 nm are effectively coupled with minor peaks at 697 and 700 nm. However, because Cr^{3+} and V^{2+} are isoelectronic and, thus, share very similar features in the emission patterns (Payne and Chase 1987; Dong-Ping et al. 1993), the possible presence of V^{2+} cannot be excluded. The emission peaks of V^{2+} at 684.9 nm

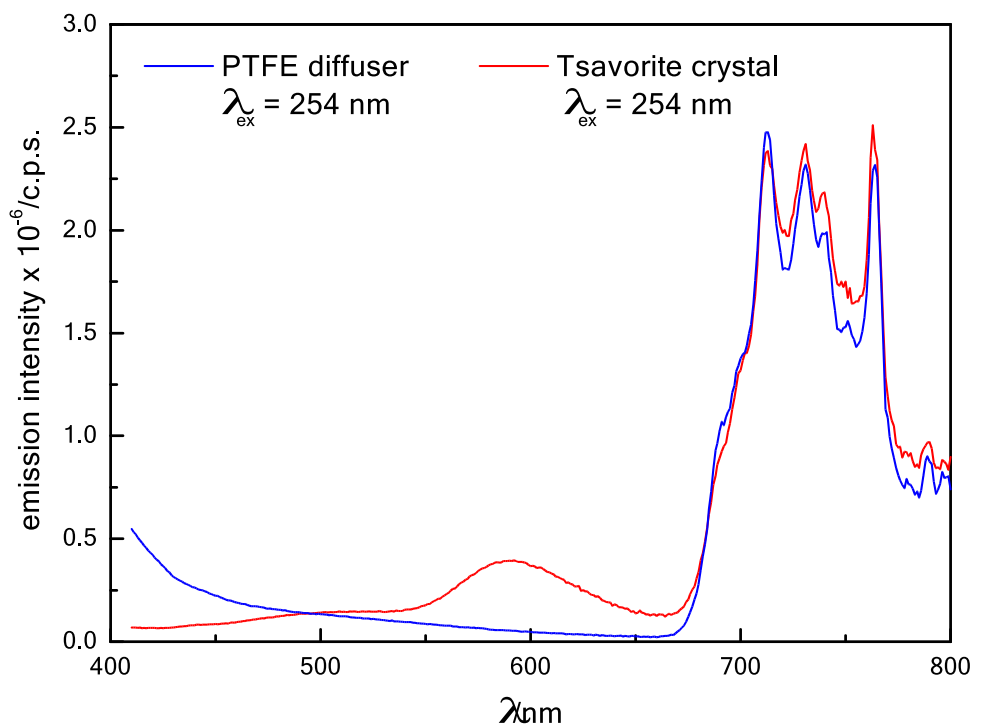
and 743.4 nm (722 nm at 80°K) were firstly identified by Schmetzer and Eysel (1974) in beryl [$\text{Be}_3\text{Al}_2\text{Si}_6\text{O}_{18}:\text{V}$], and then were used by O’Bannon et al. (2016) to discriminate, still in beryl [$\text{Be}_3\text{Al}_2\text{Si}_6\text{O}_{18}:\text{V},\text{Cr}$], the emissions of Cr^{3+} and V^{2+} . Their results show that the peaks at 691.13 and 731.55 nm ($\lambda = 532$ nm) could be attributed to V^{2+} , and at the same time an indicative example of the 675–750 nm spectral region, consisting of complex pair emission lines due to interactions between Cr^{3+} and V^{2+} , is represented.

Another interpretation comes from Gaft and Panczer (2013), due to the similarity of absorption spectra between artificial gadolinium gallium garnet activated by V^{2+} (GGG:V) and tsavorite. Gaft and Panczer (2013) attribute to V^{2+} the peaks at 704.6 and 718.8 nm, although strong differences are present between the emission spectra of GGG:V and tsavorite. On the other hand, the work of Sturge (1963), re-investigated by Palanza et al. (2010), shows that heavy irradiation of corundum [$\text{Al}_2\text{O}_3:\text{V}^{3+}$] produces only an emission doublet at 854.8–856.9 nm attributable to V^{2+} in octahedral coordination.

From the crystal chemistry standpoint, the oxidation state of V in grossular was investigated using XANES spectroscopy (Bordage et al. 2010), clarifying that V occurs only as V^{3+} and replaces Al^{3+} forming a slightly distorted octahedron with respect to the unsubstituted grossular. A different result was obtained by Righter et al. (2011) with various oxidation states of V (i.e. +2, +3 and +4) found in pyrope garnet.

Finally, considering the complexity of V emissions (Hauser and Güdel 1982) and the co-existence of

Fig. 10 Emission spectrum of a tsavorite crystal sample (red line) obtained exciting at 254 nm and stray light contribution (blue line) at 254 nm recorded with a PTFE diffuser. Bands at wavelengths longer than 670 nm are due to Xe lamp scattered light



isoelectronic Cr^{3+} , the presence of V^{2+} in our tsavorite samples can neither be confirmed nor excluded. According to O'Bannon and Williams (2022), low-temperature spectral measurements could be useful in recognising the V^{2+} emission signal.

Conclusions

A mineralogical study of natural fluorescent grossular garnet var. tsavorite has been proposed with the aim to describe this visible phenomenon that is uncommon among the garnet supergroup minerals. The samples used for the study come from the well-known Merelani Hills, Tanzania, that is the most important source of the gem grade specimen of tsavorite. The PXRD analysis has confirmed that the structure is cubic with the cell parameter very close to grossular. The application of the electron density map (also called Fourier map) has allowed to identify where the most important atomic substitution occurs in the cell with respect to a standard phase. In the case of tsavorite a positive electron density is clearly recognizable in the *Y* octahedral site, Wyckoff position 16a, indicating the substitution of Al by elements with a greater atomic number. Importantly, no excess or deficit of electron density arises in unexpected position in the cell, indicating that the photoluminescence features are specific of the crystal nature of tsavorite and not by defect or impurities. The chemical analysis has shown that vanadium (as V^{3+}) is the main element in partial substitution of Al in the standard grossular composition, and very subordinate elements are present in the order $\text{Ti} > (\text{Fe}^{2+} + \text{Fe}^{3+}) > \text{Cr}$. The calculations of the garnet end-member composition have pointed out to grossular as major phase, up to 93 mol %, followed by goldmanite $[\text{Ca}_3\text{V}_2(\text{SiO}_4)_3]$, up to 4 mol %. The fluorescence of the tsavorite crystal is easily recognizable with a commercial portable UV lamp; using a source emitting at ~ 400 nm the crystal becomes deep orange with a pink hue, while lighting with a shortwave UV lamp at ~ 280 nm the crystal becomes yellow. The photoluminescence analysis has shown that there are at least two emitting sources: (i) a band at 592 nm caused by Mn^{2+} replacing Ca^{2+} in the dodecahedral X site; (ii) a complex spectral area marked by narrow peaks where the most intense emissions are located at 701 and 716 nm. The emitting centres of these lines are probably associated to trace amounts of Cr^{3+} or, following another interpretation (Gaft and Panczer 2013), to V^{2+} , both cations substituting for Al^{3+} . Finally, while the characteristic green mint colour of tsavorite in the daylight is due to the presence of V^{3+} and Cr^{3+} (Feneyrol et al. 2014), Mn^{2+} plays the key role in the visible fluorescence phenomena. Commercially available LEDs or low-cost semiconductor lasers

emitting violet light at 405 nm are the preferred devices to observe the luminescence features of tsavorite. In fact, these devices are able to induce a strong orange luminescence, determined by the emission band at 592 nm with a contribution from the red emission in the 700 nm region, and with only a minimal interference by the exciting scattered light which is at the lower wavelength margin of the photopic visibility curve of the human eye and that, at most, would yield a pinkish hue to the perceived colour. With the help of these extremely simple and low-cost irradiation sources the identification of tsavorite in rocks would be attained simply by naked eye observation under subdued light, without the aid of any spectroscopic equipment. As well, a commercial portable UV lamp can be used as diagnostic tool for recognition of faceted tsavorite gems. As ideal prosecution of this research, the combination of trace element analysis, time resolved luminescence and Raman spectroscopy could be effective to deepening the comprehension of the garnet photoluminescence. For instance, the role of Fe^{2+} as fluorescence quencher in garnet (Liu et al. 2020).

Supplementary Information The online version contains supplementary material available at <https://doi.org/10.1007/s00269-023-01233-w>.

Acknowledgements The authors thank “Fondazione di Sardegna” for supporting the research with the fund to S. Naitza and F. Frau (CUP F75F21001270007). A. Idini wishes to thank G.B. Idini for his valuable support.

Author contributions AI: original idea, conceptualization, first draft of the manuscript, analysis and interpretation of crystallographic and elemental data, critical observations. CA: conceptualization, critical observations. FF: conceptualization, analysis and interpretation of crystallographic and elemental data, critical observations. GE: analysis and interpretation of crystallographic and elemental data. SN: overall comments on manuscript. GBDG: overall comments on manuscript. RA: analysis and interpretation of spectroscopic data.

Funding Open access funding provided by Università degli Studi di Cagliari within the CRUI-CARE Agreement.

Data Availability Data, including PXRD raw patterns, will be made available on request.

Declarations

Conflict of interest The authors declare that no conflict of interest exists.

Open Access This article is licensed under a Creative Commons Attribution 4.0 International License, which permits use, sharing, adaptation, distribution and reproduction in any medium or format, as long as you give appropriate credit to the original author(s) and the source, provide a link to the Creative Commons licence, and indicate if changes were made. The images or other third party material in this article are included in the article's Creative Commons licence, unless indicated otherwise in a credit line to the material. If material is not included in the article's Creative Commons licence and your intended use is not permitted by statutory regulation or exceeds the permitted use, you will

need to obtain permission directly from the copyright holder. To view a copy of this licence, visit <http://creativecommons.org/licenses/by/4.0/>.

References

- Adamo I, Diella V, Pezzotta F (2012) Tsavorite and other grossulars from Itrafo. *Madagascar Gems Gemol* 48(3):178–187. <https://doi.org/10.5741/GEMS.48.3.178>
- Bordage A, Brouder C, Balan E, Cabaret D, Juhin A, Arrio MA, Saintavit P, Calas G, Glatzel P (2010) Electronic structure and local environment of substitutional V^{3+} in grossular garnet $Ca_3Al_2(SiO_4)_3$: K-edge X-ray absorption spectroscopy and first-principles modeling. *Am Min* 95(8–9):1161–1171. <https://doi.org/10.2138/am.2010.3432>
- Boultif A, Louër D (2004) Powder pattern indexing with the dichotomy method. *J Appl Crystallogr* 37:724–731. <https://doi.org/10.1107/S0021889804014876>
- Bridges CR (1974) Green grossularite garnets ('tsavorites') in East Africa. *Gems Gemol* 14(10):290–295
- Cairncross B (2020) Connoisseur's choice: Tsavorite, the green gem variety of grossular, Merelani Hills, Manyara District, Tanzania. *Rocks Miner* 95(3):252–259. <https://doi.org/10.1080/00357529.2020.1716171>
- Degen T, Sadki M, Bron E, König U, Nénert G (2014) The high score suite. *Powder Diffr* 29:S13–S18. <https://doi.org/10.1017/S0885715614000840>
- Dong-Ping M, Xiao-Yi H, Ju-Rong C, Yan-Young L, Ji-Ping Z (1993) Calculations of R-line thermal shift of $MgO:V^{2+}$. *Phys Rev B* 48(19):14067–14071. <https://doi.org/10.1103/PhysRevB.48.14067>
- Feneyrol J, Giuliani G, Ohnenstetter D, Le Goff E, Malisa EPJ, Saul M, Saul E, Saul J, Pardieu V (2010) Contrôles lithostratigraphique et structural des gisements de « tsavorite » de Lemshuku, région de Merelani. *Tanzanie CR Geosci* 342(10):778–785. <https://doi.org/10.1016/j.crte.2010.06.003>
- Feneyrol J, Ohnenstetter D, Giuliani G, Fallick AE, Rollion-Bard C, Robert JL, Malisa EP (2012) Evidence of evaporites in the genesis of the vanadian grossular "tsavorite" deposit in Namalulu. *Tanzania Canad Mineral* 50(3):745–769. <https://doi.org/10.3749/canmin.50.3.745>
- Feneyrol J, Giuliani G, Ohnenstetter D, Fallick AE, Martelat JE, Monié P, Dubessy J, Rollion-Bard C, Le Goff E, Malisa E, Rakoton-drazafy AFM, Pardieu V, Kahn T, Ichang'i D, Venance E, Voarintsoa NR, Ranatsenho MM, Simonet C, Omito E, Saul M (2013) New aspects and perspectives on tsavorite deposits. *Ore Geol Rev* 53:1–25. <https://doi.org/10.1016/j.oregeorev.2013.01.016>
- Feneyrol J, Giuliani G, Ohnenstetter D, Rondeau B, Fritsch E, Fallick AE, Ichang'i D, Omito E, Rakoton-drazafy M, Ranatsenho M, Lallier F (2014) New typology and origin of tsavorite based on trace-element chemistry. *Eur J Mineral* 26(2):293–308. <https://doi.org/10.1127/0935-1221/2014/0026-2367>
- Feneyrol J, Giuliani G, Demaiffe D, Ohnenstetter D, Fallick AE, Dubessy J, Martelat JE, Rakoton-drazafy AFM, Omito E, Ichang'i D, Nyamai C, Wamunyu AW (2017) Age and origin of the tsavorite and tanzanite mineralizing fluids in the neoproterozoic Mozambique metamorphic belt. *Canad Mineral* 55(4):763–786. <https://doi.org/10.3749/canmin.1600085>
- Gaft M, Panczer G (2013) Laser-induced time-resolved luminescence spectroscopy of minerals: a powerful tool for studying the nature of emission centres. *Min Petrol* 107(3):363–372. <https://doi.org/10.1007/s00710-013-0293-3>
- Gaft M, Yeates H, Nagli L, Panczer G (2013) Laser-induced time resolved luminescence of natural grossular $Ca_3Al_2(SiO_4)_3$. *J Lumin* 137:43–53. <https://doi.org/10.1016/j.jlumin.2012.11.015>
- Gaft M, Reisfeld R, Panczer G (2015a) Interpretation of luminescence centers. In: *Modern luminescence spectroscopy of minerals and materials*, pp. 221–420. Springer Mineralogy. Springer Cham. https://doi.org/10.1007/978-3-319-24765-6_5
- Gaft M, Reisfeld R, Panczer G (2015b) Luminescent minerals. In: *Modern Luminescence Spectroscopy of Minerals and Materials*, pp. 45–219. Springer Mineralogy. Springer Cham. https://doi.org/10.1007/978-3-319-24765-6_4
- Geiger CA, Armbruster T (1997) $Mn_3Al_2Si_3O_{12}$ spessartine and $Ca_3Al_2Si_3O_{12}$ grossular garnet: structural dynamics and thermodynamic properties. *Am Min* 82:740–747
- Grew ES, Locock AJ, Mills SJ, Galuskina IO, Galuskin E, Hålenius U (2013) IMA report: nomenclature of the garnet supergroup. *Am Min* 98(4):785–810. <https://doi.org/10.2138/am.2013.4201>
- Hauser A, Gudel HU (1982) Single-crystal absorption and emission spectra of $CsVCl_3$ and $CsMgCl_3:V^{2+}$. *J Lumin* 27(3):249–256
- Jackson B (1992) Vanadian grossular garnet (tsavorite) from Pakistan. *J Gemmol* 23(2):67–70
- Jacob JB, Martelat JE, Goncalves P, Giuliani G, Devidal JL, Feneyrol J, OmitoIchang'i ED (2018) New P-T-X conditions for the formation of gem tsavorite garnet in the Voi area (southwestern Kenya). *Lithos* 320–321:250–264. <https://doi.org/10.1016/j.lithos.2018.09.010>
- Keller L, Rask J, Buseck P (1987) Arizona State University, Tempe, Arizona, USA., ICDD Grant-in-Aid
- Le Bail A (2004) Monte Carlo indexing with McMaille. *Powder Differ* 19(3):249–254. <https://doi.org/10.1154/1.1763152>
- Liu C, Chen C, Shao T, Li Z, Shen AH (2020) UV-Vis absorption spectra and 3D fluorescence spectra study of color-change garnet with red fluorescence. *Spectrosc Spect Anal* 40(7):2148–2152
- Locock AJ (2008) An Excel spreadsheet to recast analyses of garnet into end-member components, and a synopsis of the crystal chemistry of natural silicate garnets. *Comput Geosci* 34(12):1769–1780. <https://doi.org/10.1016/j.cageo.2007.12.013>
- Mazurak Z, Czaja M (1995) Optical properties of tsavorite $Ca_3Al_2(SiO_4)_3:Cr^{3+},V^{3+}$ from Kenya. *J Lumin* 65(6):335–340. [https://doi.org/10.1016/0022-2313\(95\)00086-0](https://doi.org/10.1016/0022-2313(95)00086-0)
- O'Bannon EF, Williams Q (2016) Beryl-II, a high-pressure phase of beryl: Raman and luminescence spectroscopy to 16.4 GPa. *Phys Chem Min* 43(9):671–687. <https://doi.org/10.1007/s00269-016-0837-2>
- O'Bannon EF, Williams Q (2022) High-pressure Cr^{3+} R-line luminescence of zoisite and kyanite: a probe of octahedral site distortion. *Phys Chem Minerals* 49:35. <https://doi.org/10.1007/s00269-022-01211-8>
- Osanaï Y, Ueno T, Tsuchiya N, Takahashi Y, Tainosho Y, Shiraishi K (1990) Finding of vanadium-bearing garnet from the Sør Rondane Mountains. *East Antarctica Antarct Rec* 34(3):279–291
- Palanza V, Chiodini N, Galli A, Lorenzi R, Moretti F, Paleari A, Spinolo G (2010) Updating of the interpretation of the optical absorption and emission of Verneuil synthetic and natural metamorphic blue sapphire: the role of V^{2+} , V^{3+} and Cr^{2+} . *IOP Conf Ser Mater Sci Eng* 15:012087
- Payne SA, Chase LL (1987) Excited state absorption of V^{2+} and Cr^{3+} ions in crystal hosts. *J Lumin* 38:187–189
- Righter K, Sutton S, Danielson L, Pando K, Schmidt G, Yang H, Berthet S, Newville M, Choi Y, Downs RT, Malavergne V (2011) The effect of fO_2 on the partitioning and valence of V and Cr in garnet/melt pairs and the relation to terrestrial mantle V and Cr content. *Am Min* 6:1278–1290
- Schmetzer K, Eysel HH (1974) Absorptions- und emissionspektrum von V^{2+}/V^{3+} in beryllen. *Zeitschrift Für Naturforschung A* 29:1458–1460. <https://doi.org/10.1515/zna-1974-1011>

- Smith GS, Snyder RL (1979) A criterion for rating powder diffraction patterns and evaluating the reliability of powder-pattern indexing. *J Appl Crystallogr* 12(1):60–65
- Sturge MD (1963) Optical spectrum of divalent vanadium in octahedral coordination. *Phys Rev* 130(2):639–646. <https://doi.org/10.1103/PhysRev.130.639>

Xia Z, Meijerink A (2017) Ce³⁺-Doped garnet phosphors: composition modification, luminescence properties and applications. *Chem Soc Rev* 46(1):275–299. <https://doi.org/10.1039/c6cs00551a>

Publisher's Note Springer Nature remains neutral with regard to jurisdictional claims in published maps and institutional affiliations.